High operating temperature split-off band infrared detectors

A. G. U. Perera,[a] S. G. Matsik, P. V. V. Jayaweera, and K. Tennakone[b]
Department of Physics and Astronomy, Georgia State University, Atlanta, Georgia 30303

H. C. Liu and M. Buchanan
Institute for Microstructural Sciences, National Research Council, Ottawa K1A 0R6, Canada

G. Von Winckel, A. Stintz, and S. Krishna
Center for High Technology Materials, University of New Mexico, Albuquerque, New Mexico 87101

(Received 21 March 2006; accepted 10 August 2006; published online 29 September 2006)

Heterojunction interfacial work function internal photoemission detectors were used to demonstrate infrared response originating from hole transitions between light/heavy hole bands and the split-off (spin-orbit) band. A GaAs/AlGaAs heterojunction with a threshold wavelength of $\sim 20\ \mu$m indicated an operating temperature of 130 K for split-off response in the range of 1.5–5 μm with a peak D^* of 1.0×10^8 Jones. Analysis suggests that practical devices with optimized parameters are capable of achieving room temperature operation with higher specific detectivity. Possible approaches to tailor the threshold for the split-off response to different wavelength ranges using different materials such as phosphides and nitrides are also discussed. © *2006 American Institute of Physics*. [DOI: 10.1063/1.2358106]

The room temperature detection of infrared radiation is becoming important owing to the necessity of such detection techniques in a wide range of applications in the civilian, industrial, medical, astronomy, and military sectors. Based on a well developed material system, GaAs/AlGaAs based heterojunction interfacial work function internal photoemission (HEIWIP) detectors and quantum well infrared (QWIP) detectors for mid-infrared (MIR) ($\lambda \sim 5-25\ \mu$m) to far-infrared (FIR) ($\lambda > 25\ \mu$m) ranges have been demonstrated elsewhere.[1–3] One of the major constraints on the operating temperature of IR detectors is the need for a low dark current level to obtain reliable detection. In semiconductor devices, the dark current typically increases with temperature. Hence, the dark current limit effectively determines the operating temperature of a detector.

Split-off band effects have been observed in the emission of GaAs metal semiconductor field effect transistors[4] and have enhanced the response of GaInAsP quantum wells.[5] This letter describes near-infrared (NIR) ($\lambda < 5\ \mu$m) response observed from the split-off (SO) band of GaAs/AlGaAs HEIWIP detectors designed for the MIR and FIR ranges.[6] The active region of the basic HEIWIP detector consists of one or more periods of a doped emitter and an undoped barrier layer. In general, the detector can have several emitter/barrier periods, sandwiched between two highly doped contacts as shown in Fig. 1(a). Depending on the doping required for Ohmic contacts, the top contact may also serve as the top emitter layer. A *p*-type band diagram for a single period of a detector is shown in Fig. 1(b). Here, the work function (Δ) is given by $\Delta=\Delta_d+\Delta_x$, where Δ_d and Δ_x are the contributions from doping and the Al fraction, respectively. The dashed lines indicate the valence-band edge if the barriers were GaAs. As the Al fraction is reduced, Δ will be limited by Δ_d, which in turn is a homojunction detector.

The HEIWIP detectors designed for the MIR and FIR ranges showed NIR response peaks. These peaks appear on top of the free carrier response region, when the spectral sensitivity matches the GaAs SO energy difference in the GaAs emitter based HEIWIPs. These relatively strong SO responses can be seen up to 130 K, while the free carrier response disappeared beyond 40 K. The SO band IR detectors can be based on four detection mechanisms, with each depending on three processes: (i) the photoabsorption which generates the excited carriers, (ii) escape of the carriers, and (iii) the sweep out and collection of the escaped carriers. By having a high enough doping to have the scattering length similar to the emitter thickness, the carriers will scatter before the wave function can interfere with itself and hence will not form discreet quantum states inside the well. This makes the carrier distribution in the emitter three dimensional but still bound. For doping values used in these detectors the scattering length[7] is about 200 Å, close to the thickness of the emitter. The absorption involves free carrier transitions, which is different from the response observed

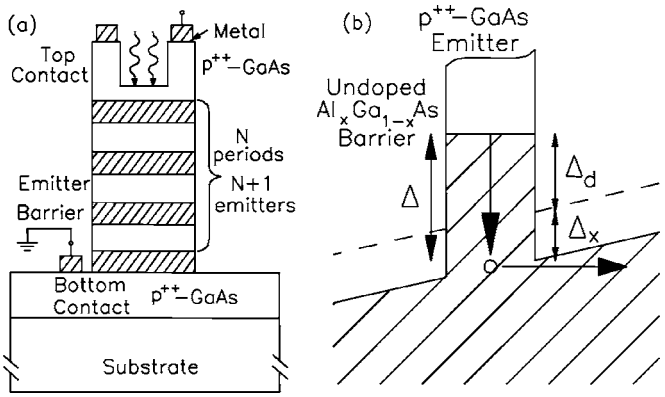

FIG. 1. (a) Typical structure of a GaAs emitter AlGaAs barrier HEIWIP detector. (b) Band diagram showing the work function (Δ) for photoemission of carriers. Here, Δ is given by $\Delta=\Delta_d+\Delta_x$, where Δ_d and Δ_x are the contributions from the doping and the Al fraction, respectively. The dashed lines indicate the valence-band edge if the barriers were GaAs.

[a]Electronic mail: uperera@gsu.edu
[b]Also at Institute of Fundamental Studies, Hantana Road, Kandy, Sri Lanka.

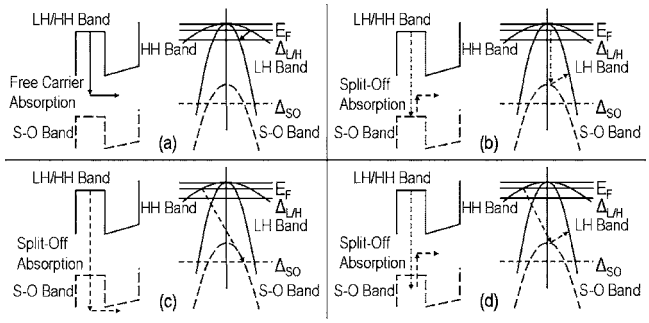

FIG. 2. Band diagram of the hole bands [light hole (LH) and heavy hole (HH)] and an energy diagram illustrating (a) the standard HEIWIP response mechanism and [(b)–(d)] the split-off (SO) band mechanisms. The SO response can be categorized as (b) direct absorption, (c) indirect absorption without scattering, and (d) indirect absorption with scattering. Actions involving the SO band as either the initial or final state are indicated by dashed arrows. The horizontal lines indicate the barrier ($\Delta_{L/H}$ and Δ_{SO} for the LH/HH and SO holes, respectively) and Fermi (E_F) energies.

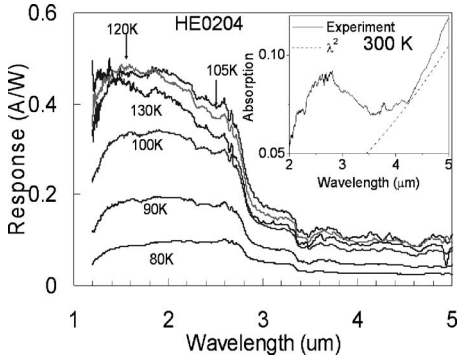

FIG. 3. Measured responsivity of HE0204 at various temperatures at 5 kV/cm. The inset shows the measured absorption for the sample showing the increased absorption from the split-off response. The dashed line shows expected free carrier response as a λ^2 curve.

previously in Si/SiGe detectors[8] which used transitions from bound states to either a bound split-off band state or a continuum state which is a mixture of the light, heavy, and split-off hole bands. The Si/SiGe detectors are QWIPs operating in a bound-bound and bound-continuum mode. In explaining the detection mechanisms, three bands will have to be considered: the light hole (LH) and heavy hole (HH) bands, which are degenerate at $k=0$, and the SO band, which is separated from them by an energy E_{SO}. Under equilibrium conditions, a p-doped region will have a Fermi level in the LH and HH bands, but above the SO band maximum. The four detection mechanisms include the standard free carrier absorption described[9] before and used in both homojunction[10] and heterojunction[11] detectors. The other three mechanisms can only occur for p-type detectors as they involve transitions between the hole bands. Once the carrier is in the SO band, it can escape directly or scatter back into the LH/HH bands, and then escape.

(1) As seen in Fig. 2(a), for free carrier absorption in the emitter layers, the carriers remain in the LH/HH band. The excited carriers then escape from the emitter layer by internal photoemission at the interface between the emitters and barriers.
(2) If the transition between the LH/HH band and the SO band is direct, as shown in Fig. 2(b), the final energy of the excited carrier will not allow it to escape from the emitter while remaining in the SO band. This is due to the energy of states in the SO band with $k<k_F$, where k_F corresponds to the Fermi level in the heavy hole band being above the barrier in the SO band. The carrier will scatter out of the SO band back to the LH/HH band with an excited energy, and then will be able to escape by a process via the standard mechanism. Because of the occupation in the LH/HH bands, this scattering time should be faster than a direct relaxation.
(3) For an indirect transition, it is possible for the excited carrier to have $k>k_F$, which means that the carrier can have sufficient energy to escape directly in the SO band [Fig. 2(c)]. In this case the escape process will be similar to that of the standard mechanism.
(4) For indirect transitions in which the carriers do not end up in the escape cone [Fig. 2(d)], it is still possible to go through the scattering process as in mechanism 2 in order to escape. Here process A is an indirect photoabsorption, followed by a scattering event to the LH or HH band. The internal photoemission then occurs in the LH or HH band. This process provides an additional escape route for carriers in mechanism 3 that are not in the escape cone as well as carriers resulting from absorption of lower energy photons that would not have any possibility of escape in the SO band. The threshold here is determined by the difference between the Fermi energy and the SO band edge.

Two groups of detectors were used in this study. The SO response is first shown using a detector designed for the 10–15 μm range with a 20 μm threshold,[2] which was not designed for optimum SO response. The detector HE0204 design consisted of 16 periods of p-doped 188 Å GaAs emitters doped to 10^{18} cm^{-3} with carbon and 1250 Å $Al_{0.12}Ga_{0.88}As$ barriers. The top and bottom contacts were 1×10^{19} cm^{-3} p-doped GaAs layers with 0.2 and 0.7 μm thicknesses, respectively. The processed detector is shown in Fig. 1(a).

The measured responsivity in the 1.2–5 μm SO range for HE0204 at 79–130 K is shown in Fig. 3. A peak response of 0.45 A/W was seen at 105 K at 2.0 μm. As the temperature was further increased, the response decreased and was not measured beyond 130 K. The increase in response with temperature may be related to phonon effects on the escape rate for excited carriers. Further studies to investigate the temperature dependence are planned. The total quantum efficiency determined by dividing the photocurrent by the incident photon rate was ~27, and at 1.8 μm a specific detectivity (D^*) of 2.2×10^7 Jones was obtain at 90 K. This value is low due to the design of these detectors for operation at much lower temperatures. The increased barrier in an optimized detector should reduce the dark current and hence improve D^*. The two steps seen in the response at 2.8 and 3.4 μm are probably caused by the thresholds for mechanisms 3 and 2/4, respectively. This indicates that the use of high doping is the preferred approach. A small signature could be identified at 3.7 μm, which could possibly be a signature of the bound heavy-light hole to bound SO transitions.

Based on previous experimental results and the standard thermionic current calculations, the dark current should not increase significantly, as doping is increased until the defect

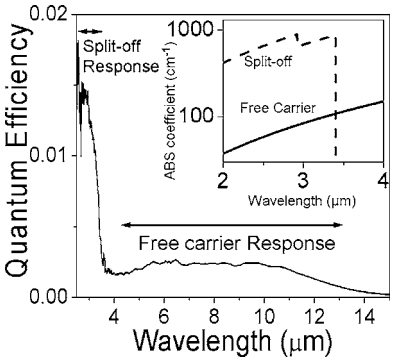

FIG. 4. Quantum efficiency of detector 1332 at 50 K at 3 kV/cm. The inset shows the calculated absorption coefficient for the free carrier and the SO band absorptions in a 3×10^{18} cm^{-3} p-doped GaAs layer.

assisted tunneling dominates. If the doping is kept below these high values, the absorption is increased; therefore the response and hence the background limited infrared photodetection temperature should increase.

The detector 1332 had 16 periods with 3.6×10^{18} and 1.2×10^{18} cm^{-3} Be-doped top contact and emitters, respectively. The quantum efficiency of detector 1332 at 50 K and a bias field of 3 kV/cm is shown in Fig. 4. The broad response from 5–15 μm is due to the free carrier absorption and the sharp peak at 2–4 μm is due to the SO response. This increased quantum efficiency is due to the increased absorption/emission in the SO region. For free carrier and indirect absorption response (2, 3, and 4), a phonon or an impurity scattering event is required in the absorption to conserve momentum, while in mechanisms 2 and 4, a scattering event is also required. Since mechanism 4 requires two extra particles, it should be slower than the other three. The threshold for mechanism 3 will be shorter than for mechanisms 2 and 4 due to the requirement of passing the barrier in the SO band. Based on the width and two thresholds in the SO response, both the direct and indirect absorptions occur in the SO response.

In order to understand the strong response observed using the SO band, calculations were carried out to determine the relative absorptions for the free carrier and SO responses. The first step was to use a $\mathbf{k}\cdot\mathbf{p}$ model, similar to that used in quantum dots,[12] and quantum wells to calculate the LH, HH, and SO hole energy bands. The absorption coefficient was then calculated as a function of photon energy $\hbar\omega$ from the energy states in the band. The calculation was done for a 1 μm thick GaAs layer that was p doped to 1×10^{18} cm^{-3}. The absorption by the SO band was over an order of magnitude larger than for the free carrier absorption in the LH/HH bands as shown in the inset to Fig. 4, indicating the relative improvement of the SO mechanism in this range. As shown in the inset to Fig. 3 the measured absorption is increased in the split-off region compared to the expected free carrier absorption. The experimental quantum efficiency is larger than the calculated quantum efficiency (even with the increased experimental absorption taken into account). This difference is believed to be due to the gain resulting from the large split-off energy (~340 meV) for GaAs. The high energy for carriers that have been excited into the split-off band means that they will have sufficient energy to excite additional carriers via impact effects, introducing a high gain factor into the detectors. The step seen in response at 3.4 μm is in good agreement with the calculated results shown in the inset to Fig. 4. However, there is a small discrepancy with the drop calculated to occur at 2.9 μm. The experimental step is ~0.15 μm wide (possibly due to the effects of the photoemission process), and the threshold may be longer than it appears in Fig. 3.

The tested devices with a threshold of ~20 μm showed a maximum operating temperature of 130 K. By reducing the threshold to ~5 μm, the operating temperature should be increased to 300 K with D^* of $\sim5\times10^9$ Jones. The response can be optimized by increasing the number of layers in order to get increased absorption using surface plasmon resonances in metallic nanoparticles deposited on the detector surface.[13] Properly optimized device working at room temperature may compete with currently available uncooled detectors.[14] Materials other than GaAs/AlGaAs may lead to improved coverage of the 3–5 μm range. A direct transition to the SO band for InP gives a threshold of 11 μm, while the nitride materials may be able to operate at 60 μm or beyond in the SO mode. The research will look at which materials are optimal for use in the different spectral ranges, with the emphasis on the 10–15 μm range for which the phosphides should be best.

This work is supported by the NSF under Grant Nos. ECS 05-53051 and INT-0322355.

[1] M. Jhabvala, K. Choi, A. C. Goldberg, A. T. La, and S. D. Gunapala, Proc. SPIE **5167**, 175 (2004).
[2] S. G. Matsik, M. B. M. Rinzan, D. G. Esaev, A. G. U. Perera, H. C. Liu, and M. Buchanan, Appl. Phys. Lett. **84**, 3435 (2004).
[3] M. B. M. Rinzan, A. G. U. Perera, S. G. Matsik, H. C. Liu, Z. R. Wasilewski, and M. Buchanan, Appl. Phys. Lett. **86**, 071112 (2005).
[4] K. S. Zhuravlev, V. A. Kolosanov, A. G. Milekhin, V. G. Polovinkin, T. S. Shamirzaev, Yu N. Rakov, Yu B. Myakishev, J. Fryar, E. McGlynn, and M. O. Henry, Semicond. Sci. Technol. **19**, S94 (2004).
[5] J. R. Hoff, M. Razeghi, and G. J. Brown, Phys. Rev. B **54**, 10773 (1996).
[6] D. G. Esaev, M. B. M. Rinzan, S. G. Matsik, and A. G. U. Perera, J. Appl. Phys. **96**, 4588 (2004).
[7] J. Maserjian, Proc. SPIE **1540**, 127 (1991).
[8] R. P. G. Karunasiri, J. S. Park, and K. L. Wang, Appl. Phys. Lett. **62**, 2434 (1992).
[9] A. G. U. Perera, H. X. Yuan, and M. H. Francombe, J. Appl. Phys. **77**, 915 (1995).
[10] A. G. U. Perera, W. Z. Shen, H. C. Liu, M. Buchanan, M. O. Tanner, and K. L. Wang, Appl. Phys. Lett. **72**, 2307 (1998).
[11] A. G. U. Perera, S. G. Matsik, B. Yaldiz, H. C. Liu, A. Shen, M. Gao, Z. R. Wasilewski, and M. Buchanan, Appl. Phys. Lett. **78**, 2241 (2001).
[12] H. Jiang and J. Singh, Phys. Rev. B **56**, 4696 (1997).
[13] D. M. Schaadt, B. Feng, and E. T. Yu, Appl. Phys. Lett. **86**, 063106 (2005).
[14] A. Rogalski, Opto-Electron. Rev. **12**, 221 (2004).